Angle-dependent magnetic-relaxation studies in single-crystal $YBa_2Cu_4O_8$

D. Zech, H. Keller, M. Warden, H. Simmler, B. Stäuble-Pümpin, and P. Zimmermann
Physik-Institut der Universität Zürich, CH-8001 Zürich, Switzerland

E. Kaldis and J. Karpinski
Laboratorium für Festkörperphysik Eidgenössiche Technische Hochschule Zürich, CH-8093 Zürich, Switzerland

(Received 18 February 1993)

The relaxation behavior of the remanent magnetization *vector* $\mathbf{M}_R$ in single-crystal $YBa_2Cu_4O_8$ was studied as a function of the orientation angle between the c axis and the external field by measuring the time dependence of the components of $\mathbf{M}_R$ parallel and perpendicular to the c axis. At low temperatures ($T/T_c < 0.55$) a rotation of $\mathbf{M}_R$ towards the c axis is observed for all orientation angles. For $T/T_c > 0.55$ and the initial external field not parallel to the c axis $\mathbf{M}_R$ turns towards the ab plane both in time and with temperature. It is suggested that the unusual relaxation behavior may be associated with a dimensional crossover from 2D to 3D superconducting behavior.

I. INTRODUCTION

Soon after the discovery of the cuprate high-T_c superconductors, considerable attention was directed to the anisotropic properties of these materials. For uniaxial superconductors, such as the layered cuprate systems, the anisotropy is expressed by the parameter γ, which, according to the anisotropic Ginzburg-Landau (GL) theory, is related to the effective-mass ratio by $\gamma=(m_c^*/m_{ab}^*)^{1/2}$, where m_c^* and m_{ab}^* denote the effective masses in the c direction and the ab plane, respectively.[1-4] As a consequence, the penetration depth λ and the coherence length ξ are also anisotropic and the flux lattice shows a more complicated structure than for isotropic superconductors, which is still not completely understood (Refs. 2-7). The origin of this anisotropy in cuprate superconductors is due to the layered structure of these materials. Although the coherence length in the c direction ξ_c, is, in general, much larger than the spacing between adjacent CuO_2 layers, for temperatures near T_c, the value of ξ_c at low temperatures may, in certain cases, be less than the distance between adjacent layers.[8] As a result, at low temperatures, superconductivity is restricted predominantly to the two-dimensional (2D) CuO_2 layers. Consequently, the superconducting carrier density n_s is modulated along the c direction. In this case, the vortex structure is not well described by the three dimensional (3D) anisotropic GL or London theory both of which assume no spatial variation of n_s along a vortex line and the superconducting CuO_2 planes are coupled by Josephson junctions as described by the Lawrence-Doniach model (LD).[9,5,6] Although the vortex structure of a system consisting of weakly coupled superconducting layers is still controversial, the vortex dynamics in a LD-type superconductor is expected to be significantly different from that of an anisotropic 3D GL-type superconductor. Because ξ_c increases with temperatures, a dimensional crossover from quasi-2D to 3D superconducting behavior is expected to occur around a certain crossover temperature due to the increasing coupling strength between adjacent layers.[10,11] For example, experimental evidence of a 2D-3D crossover has been observed in the temperature dependence of H_{c2} in superconducting multilayers.[12] This crossover should also give rise to a distinct change in the vortex dynamics. Note that the GL effective-mass anisotropy is only well defined for 3D anisotropic superconductors. For 2D superconductors a revised interpretation of γ and m_c is required. As an example, for $Bi_2Sr_2CaCu_2O_8$ magnetization and torque experiments performed very close to T_c (Refs. 13,14) cannot be explained within the framework of the 3D anisotropic GL theory. A dimensional crossover from 2D to 3D behavior in $Bi_2Sr_2CaCu_2O_8$ is expected to occur very close to T_c, where thermal fluctuations prevent a direct observation. On the other hand, the small anisotropy of $YBa_2Cu_3O_{7-\delta}$($\gamma\approx 5$) makes a direct observation of a 2D-3D crossover very difficult[10] due to the broad temperature regime where this crossover should take place. As will be demonstrated here, the anisotropy of $YBa_2Cu_4O_8$ lies in a suitable range ($\gamma\approx 10$) (Refs. 14,15) to make an observation of a dimensional crossover possible (see Sec. IV).

In this paper magnetic-relaxation measurements on a single crystal of $YBa_2Cu_4O_8$ are presented as a function of temperature and orientation angle θ between the c axis and the applied magnetic field. The possibility to measure the magnetization vector, using two independent superconducting quantum interference device SQUID sensors, provided information on the relaxation of the angle between the remanent magnetization and the c direction, in addition to common magnetic-relaxation studies of the magnitude of the remanent magnetization. At present the influence of twin boundaries, impurities, oxygen deficiencies, granularity, and coupling between adjacent CuO_2 layers on the magnetic relaxation in cuprate high-T_c systems is unclear. For a deeper understanding of the flux-line dynamics in these systems, high-quality single-crystal samples are required. From this point of view, single crystal $YBa_2Cu_4O_8$ is an ideal candidate for magnetic-relaxation studies. Due to the double chain

0163-1829/93/48(9)/6533(6)/$06.00

structure of this material, the crystallographic axes are well defined over the entire sample, and no twin boundaries are present, which could affect the relaxation behavior in an unpredictable way. In addition, $YBa_2Cu_4O_8$ is thermally stable, shows no oxygen deficiency, and in a single crystal there are no intergranular weak links.

The organization of the paper is as follows. In Sec. II we briefly describe the experimental details and discuss the theoretical background of flux creep, insofar as that is relevant to the analysis and interpretation of the present experiments. The results of the angle dependent magnetic-relaxation experiments in single crystal $YBa_2Cu_4O_8$ are presented in Sec. III. In the conclusion given in Sec. IV, the experimental results are discussed in the framework of current models of flux-line structure in extreme type-II layered superconductors and in terms of a possible dimensional crossover from 2D to 3D behavior.

II. EXPERIMENTAL DETAILS

The high-quality $YBa_2Cu_4O_8$ single crystal used in this study was grown at the ETH Zürich, by a high-pressure flux method described elsewhere.[16,17] The platelike sample had an approximate size of $1\times1\times0.1$ mm^3 with the c axis perpendicular to the plate and a mass of 0.57 mg. Magnetization measurements in a low-magnetic field (1 mT) showed a sharp transition at 74.1 K (onset) with a width of 3K (10–90)%. This value of T_c is somewhat lower than those usually found for polycrystalline material ($T_c \simeq 81$ K).[18] The magnetic-relaxation measurements were performed with a Quantum Design SQUID magnetometer. The apparatus is equipped with two independent SQUID sensors, allowing a simultaneous measurement of the longitudinal and transverse components of the magnetization *vector* **M** with respect to the applied magnetic field along the z axis (see Fig. 1). The signal-to-noise ratio of the SQUID sensors was improved by an order of magnitude by using an active magnetic-field compensation system that minimized disturbing effects from surrounding stray fields. A sample holder made out of quartz glass was developed, which allowed a precise orientation of the single crystal in the external magnetic field. The orientation angle θ was measured optically using a laser with an accuracy of $\pm1°$. The relaxation behavior of the remanent magnetization was investigated as a function of the orientation angle θ and temperature T. For each experiment the crystal with fixed orientation was cooled slowly (≈5 K/min) in an external field of 50 mT to the desired temperature. When the temperature was stable, the external field was switched off at time $t=0$, and the behavior of the remanent magnetization *vector* $\mathbf{M}_R$ was studied as a function of time.

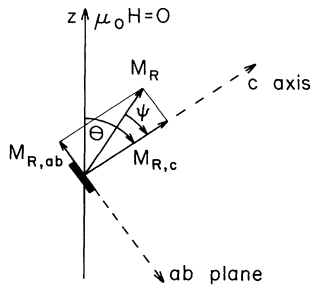

FIG. 1. Schematic representation of the sample geometry. All quantities are defined in the text. The z axis represents the direction of the external fields which was applied when the sample was cooled down.

For the data analysis we made use of the simplest flux-creep models incorporating only one effective activation energy. According to the classical Kim-Anderson model[19] of thermally activated flux creep, the decay of the magnitude of the remanent magnetization $M_R=|\mathbf{M}_R|$ is logarithmic in time. A convenient way to define a decay rate is in the form of the normalized relaxation rate S at the observation time t_b which is given by

$$S=-\frac{1}{M_R}\frac{dM_R}{d\ln(t)}\bigg|_{t=t_b} . \tag{1}$$

According to the model of Hagen, Griessen, and Salomons[20] the relaxation rate S can be expressed as follows:

$$S=\left[\frac{U_0}{k_BT}-\ln\left[\frac{t_b}{\tau}\right]\right]^{-1} . \tag{2}$$

Here U_0 is a mean activation energy and $\tau=(10^{-6}-10^{-12})$ s is a characteristic microscopic time of the relaxation process, normally associated with the flux bundle hopping. The term $\ln(t_b/\tau)$ is typically 20–34 for an observation time $t_b=600$ s. For $U_0/k_BT\gg\ln(t_b/\tau)$, this expression reduces to the well-known Kim-Anderson behavior with a linear increase of S with temperature:[19]

$$S=\frac{k_BT}{U_0} . \tag{3}$$

Note that Eq. (2) is only valid when the related relaxation process is logarithmic in time and the relaxation rate S is an increasing function of temperature. In order to explain the commonly observed maximum or plateau in S (see, for example, Ref. 21) more detailed relaxation models are required, such as models including a distribution of pinning energies[21] or glasslike decay models with a nonlogarithmic time behavior.[22,23] The maximum of S is not only a characteristic feature of cuprate superconductors, but also of other short coherence length superconductors such as Chevrel phase systems[24] or superconducting C_{60} compounds.[25]

In strongly anisotropic layered superconductors the relaxation process is very complex due to the relaxation of flux lines which for an arbitrary orientation of the external magnetic field are, in general, not parallel to a crystallographic axis and due to the temperature-dependent coupling strength between adjacent layers. The structure of an entangled flux-line lattice in either the GL or the LD model has been the subject of several papers (e.g., Refs. 2-7). However, to our knowledge, no relaxation theory of flux lines has been developed so far for these models.

A convenient way to describe the decay of the remanent magnetization $\mathbf{M}_R$ in anisotropic superconductors is to write the magnetization as an imaginary quantity $\overline{M_R}$ defined by

$$\overline{M_R}=M_R(t)e^{i\Psi(t)}\ ,$$
$$M_R(t)=M_0 r_M(t)\ , \tag{4}$$
$$\Psi(t)=\Psi_0 r_\Psi(t)\ .$$

Here $M_R(t)$ denotes the magnitude of the measured remanent magnetization vector $\mathbf{M}_R$ and $\Psi(t)$ is the angle between the remanent magnetization and the crystallographic c axis (see Fig. 1). M_0 and Ψ_0 are the initial values of $M_R(t)$ and $\Psi(t)$, and $r_M(t)$ and $r_\Psi(t)$ are the corresponding relaxation functions, respectively. The relaxation of $\mathbf{M}_R$ is, therefore, described by a rotation of $\mathbf{M}_R$ with respect to the c axis and a decay of the magnitude of $\mathbf{M}_R$. For the present work it is convenient to decompose the remanent magnetization vector $\mathbf{M}_R$ into components perpendicular ($M_{R,c}$) and parallel ($M_{R,ab}$) to the CuO_2 layers as shown schematically in Fig. 1. Using the notations defined in Eq. (4) and Fig. 1, one obtains

$$M_{R,ab}=M_R\sin(\Psi)\ ,$$
$$M_{R,c}=M_R\cos(\Psi)\ , \tag{5}$$

where both M_R and Ψ are time dependent. According to Eq. (1) the corresponding normalized relaxation rates S_c and S_{ab} are then given by

$$S_\alpha=-\frac{1}{M_{R,\alpha}}\frac{dM_{R,\alpha}}{d\ln t}\bigg|_{t=t_b}\ , \tag{6}$$

where $\alpha=c$ or ab. For a nonvanishing derivative $d\Psi/d\ln t$, it follows directly that $S_{ab}\neq S_c$. Therefore, different relaxation rates in the ab plane and along the c axis indicate a macroscopic rotation of the remanent magnetization in addition to a decay of the magnitude of $\mathbf{M}_R$. The corresponding mean effective activation $U_{0,\alpha}$ can be estimated from S_α using either Eqs. (2) or (3). To avoid the difficulties in calculating $U_{0,\alpha}$ from Eqs. (2) or (3) (due to the uncertainty of τ) we estimated values of an effective activation energy only over the temperature range where S_α increases. A rotation of $\mathbf{M}_R$ strongly affects the estimated values for $U_{0,\alpha}(\alpha=c,ab)$; a rotation toward the α direction will increase $U_{0,\alpha}$, whereas a rotation away from the α direction will decrease $U_{0,\alpha}$.

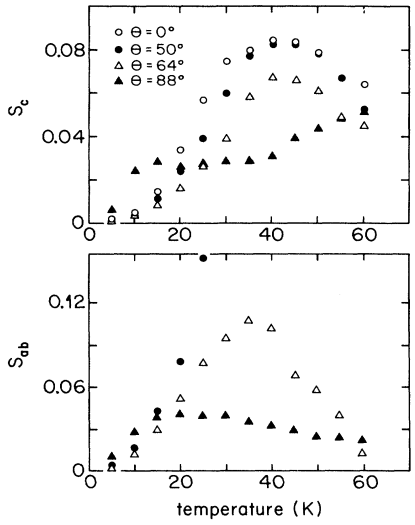

FIG. 2. Normalized relaxation rates S_c (top) and S_{ab} (bottom) as defined in Eq. (6) as a function of temperature and orientation angles $\theta=0°$, 50°, 65°, and 88° for single-crystal $YBa_2Cu_4O_8$. For $\theta°$, no remanent magnetization was measured parallel to the ab plane, and, therefore, S_{ab} is not defined.

III. EXPERIMENTAL RESULTS

Magnetic-relaxation experiments were performed as described in Sec. II in the temperature range of 5–60 K and for four orientation angles $\theta=0°$, 50°, 64°, and 88°. In Figs. 2 and 3 the corresponding normalized relaxation rates S_c and S_{ab} of the remanent magnetization determined at $t_b=600$ s are plotted as a function of temperature, and the corresponding initial values of M_0 and Ψ_0 [cf. Eq. (4)] are listed in Table I for the four orientation

TABLE I. Initial values M_0 and Ψ_0 as a function of temperature and orientation angles θ. For $\theta=0°$, M_0 was for all temperatures parallel to the c axis ($\Psi=0°$, not tabulated).

Angle	$\theta=0°$	$\theta=50°$		$\theta=64°$		$\theta=88°$	
T (K)	M_0 (10^{-3} emu)	M_0 (10^{-3} emu)	Ψ_0 (deg)	M_0 (10^{-3} emu)	Ψ_0 (deg)	M_0 (10^{-3} emu)	Ψ_0 (deg)
5	12.941	9.579	16.5	6.666	18.5	2.175	76.9
10	12.463	7.916	12.3	6.403	17.9	1.579	75.7
15	11.577	7.306	10.0	6.005	15.5	0.962	7.39
20	9.953	6.329	6.9	5.434	11.8	0.597	72.0
25	7.625	5.182	3.6	4.684	7.9	0.389	69.6
30	5.184	3.779	1.3	3.868	4.3	0.274	69.1
35	3.251	2.484	0.2	2.926	2.0	0.210	68.8
40	2.174	1.527	0.1	1.933	1.2	0.163	68.4
45	1.207	0.935	0.0	1.190	1.0	0.133	68.8
50	0.747	0.571	0.0	0.726	1.2	0.101	69.3
55	...	0.342	0.0	0.428	1.8	0.093	74.4
60	0.322	0.197	0.1	0.258	2.7	0.082	78.0

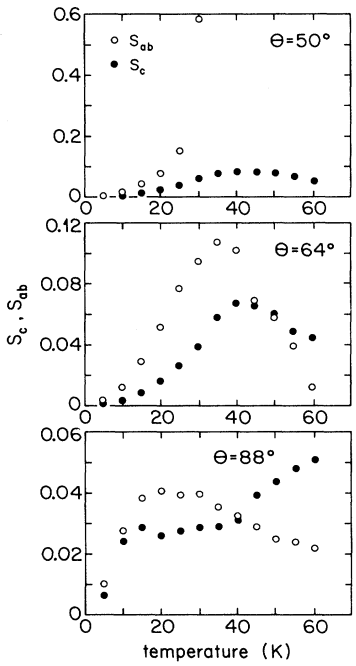

FIG. 3. Temperature dependence of the normalized relaxation rates S_c and S_{ab} for single-crystal $YBa_2Cu_4O_8$ for orientation angles $\theta=50°$, 64° and 88°. For $\theta=50°$ and $T>35$ K, no remanent magnetization in the *ab* plane was detected and, therefore, S_{ab} is not defined.

angles of θ. For $\theta=0°$ no remanent magnetization in the *ab* plane was detected ($M_{R,ab}=0$), indicating that the remanent magnetization was perfectly aligned along the *c* axis ($M_R=M_{R,c}$). The relaxation rate S_c (Fig. 2) shows a broad maximum at $T\approx40$ K for all orientations, except for $\theta=88°$, where the initial magnetic field was almost parallel to the *ab* plane. As shown in Figs. 2 and 3, however, the relaxation behavior of the remanent magnetization in the *ab* plane $M_{R,ab}$ was quite different. In the low-temperature region ($T<40$ K) S_{ab} was larger than S_c for all orientation angles of θ. As an example, for $\theta=50°$ the relaxation rate S_{ab} increases very rapidly with rising temperature, reaching a value of about 0.6 at 30 K, which is an order of magnitude larger than the corresponding value for S_c. For $T>35$ K no remanent magnetization in the *ab* plane $M_{R,ab}$ could be detected for $\theta=50°$, and thus S_{ab} is not defined. For $\theta=64°$ and 88°, on the other hand, S_c approached S_{ab} at about 40 K, and in the high-temperature region ($T>40$ K) S_c was even larger than S_{ab}.

The different temperature behavior of S_c and S_{ab} implies that the corresponding activation energies $U_{0,c}$ and $U_{0,ab}$ are also quite different. The positive curvature of $S_c(T)$ and $S_{ab}(T)$ at low temperatures observed in Figs. 2 and 3 suggests that the quantity U_0/k_BT in Eq. (2) is of the same order of magnitude as $\ln(t_b/\tau)$. In order to extract estimates of the mean effective activation energies $U_{0,c}$ and $U_{0,ab}$ from the relaxation data, we made use of the simple relations (2) and (3). The results are summarized in Table II. The values of $U_{0,c}$ range from 30–150 meV and are comparable to those reported for $YBa_2Cu_3O_{7-\delta}$.[20] Somewhat smaller effective activation energies were found for $U_{0,ab}=25$–60 meV. We further note that $U_{0,c}$ increases with increasing orientation angle θ, whereas $U_{0,ab}$ decreases. For $\theta=88°$, however, a change in the mean effective activation energy was observed at $T\simeq40$ K. This is evident from the temperature dependence of the normalized relaxation rates S_c and S_{ab} for $\theta=88°$ (Fig. 2). S_c shows a plateau in the temperature region between 20–35 K and then increases almost linearly above 40 K. A similar behavior of $S_c(T)$ was previously reported for single-crystal $Bi_2Sr_2CaCu_2O_8$ (Ref. 13) and $Tl_2Ba_2CaCu_2O_y$ (Ref. 26). For both materials the normalized relaxation rate as a function of temperature showed two pronounced peaks, which were associated with two distinct pinning barriers with different energy scales. Analyzing our data as described in Ref. 26 [using Eq. (3)] one obtains rough estimates of the corresponding effective pinning energies: $U_{0,c}\approx30$ meV for $T<25$ K and $U_{0,c}\approx100$ meV for 45 K $<T<60$ K (see Table II).

The different behavior of the relaxation rates S_{ab} and S_c (Figs. 2 and 3) as a function of temperature and orientation angle may be interpreted in terms of a slow rotation of the remanent magnetization $\mathbf{M}_R$ as a function of time (see Sec. II). The time evolution of the angle Ψ (angle between $\mathbf{M}_R$ and the *c* axis, see Fig. 1) was derived from Eqs. (4) and (5), assuming a logarithmic time dependence of $M_{R,c}$ and $M_{R,ab}$, which, indeed, was observed. In the framework of the extended Anderson model proposed by Hagen and Griessen,[21] one finds for small angles,

$$\Psi(t)\approx\frac{M_{R,ab}}{M_{R,c}}\approx\Psi_0\left[1-\left[\frac{k_BT}{U_{0,ab}}-\frac{k_BT}{U_{0,c}}\right]\ln\left[1+\frac{t}{\tau}\right]\right]. \tag{7}$$

In Fig. 4 the time dependence of Ψ is shown for $\theta=64°$ and $T=30$ and 60 K, respectively. For $T=30$ K the angle Ψ decreases with time, indicating a slow rotation of $\mathbf{M}_R$ toward the *c* axis, whereas for $T=60$ K, Ψ increases with time and $\mathbf{M}_R$ rotates away from the *c* direction. According to Eq. (7), the rotation angle Ψ is expected to vary logarithmically in time for $t/\tau\gg1$. This is clearly demonstrated in Fig. 4. For both cases, the relaxation of Ψ is in a first approximation logarithmic in time, although at 60 K the scattering of the data points is quite

TABLE II. Mean values of the effective activation energies $U_{0,c}$ and $U_{0,ab}$ for various orientation angles θ as obtained either from Eqs. (2) or (3).

θ (deg)	$U_{0,c}$ (meV)	$U_{0,ab}$ (meV)	Equation
0 ($T<40$ K)	90	...	2
50 ($T<40$ K)	95	60	2
64 ($T<40$ K)	145	25	2
88 ($T<25$ K)	30	30	3
88 ($T>45$ K)	100	...	3

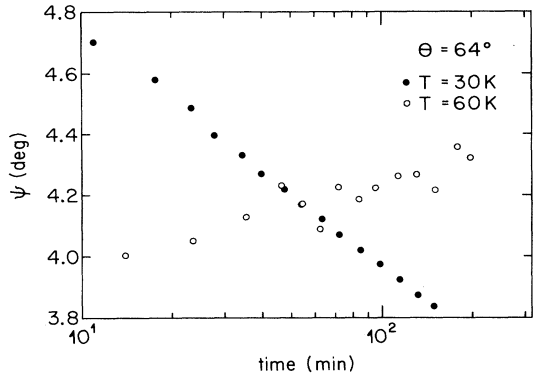

FIG. 4. Time dependence of the angle Ψ between the c axis and the remanent magnetization measured for $\theta=64°$ at 30 and 60 K, respectively. For $T=30$ K, a rotation of $\mathbf{M}_R$ towards the c axis was observed, whereas for $T=60$ K, $\mathbf{M}_R$ turned away from the c direction. In both cases a logarithmic time dependence of Ψ was observed.

large due to the weak signals. Moreover, one has to distinguish between two cases: For $U_{0,c} > U_{0,ab}$, $\Psi(t)$ decreases and the remanent magnetization $\mathbf{M}_R$ turns toward the c direction, whereas for $U_{0,c} < U_{0,ab}$, $\Psi(t)$ increases and consequently $\mathbf{M}_R$ rotates away from the c axis. Indeed, both cases were observed experimentally, as evidenced in Fig. 4.

Figure 5 shows the temperature dependence of the rotation angle Ψ determined at $t=600$ s for the orientation angles $\theta=50°$, 64°, and 88°. At low temperatures, Ψ first decreases with increasing temperature for all orientations, exhibiting a broad minimum around 40 K and then increases with increasing temperature. This behavior is observed for all three orientation angles, even for $\theta=50°$, where $\Psi(t)$ is practically zero above 40 K. Finally, we note that for $T>40$ K, the remanent magnetization $\mathbf{M}_R$ remains parallel to the c axis only for $\theta=0°$. For $\theta=50°$, 64°, and 88°, on the other hand, $\mathbf{M}_R$ turns towards the ab plane and Ψ increases with temperature at $t=600$ s.

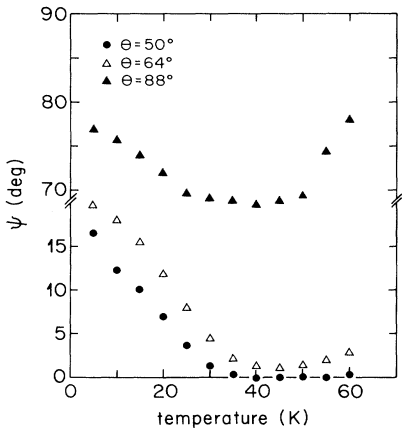

FIG. 5. Temperature dependence of the angle Ψ between the c axis and the remanent magnetization determined at $t=600$ s for the $\theta=50°$, 64°, and 88°.

IV. CONCLUSIONS

The results described above cannot be explained in terms of a classical flux-creep model. In the cuprates, the vortex structure and dynamics are very complex. Several models have been proposed in order to describe the vortex structure in these systems. For example, anistropic London and Ginzburg-Landau (GL) models,[1–4] including a phenomenological anisotropic effective-mass tensor, and Lawrence-Doniach-type (LD) models.[9,5,6] When the external magnetic field is parallel to the c axis both classes of models predict essentially the same overall vortex structure. However, for an arbitrary field orientation, the intrinsic structure of a vortex core looks quite different for the two types of models. In the GL case, a vortex line is a 3D object, whereas in the LD models, 3D vortex lines are formed by stacks of coupled 2D vortices (pancake vortices) confined to the layers. So far, no flux-creep theories (either for the GL or LD model) have been developed describing the vortex dynamics in strongly layered superconductors for an arbitrary orientation angle of the external magnetic field.

In the following we discuss the relaxation experiments presented in Sec. III. When the external magnetic field is switched off, the superconductor relaxes to the thermodynamic equilibrium state which can be reached via different decay channels: (i) decay of the remanent magnetization $\mathbf{M}_R$ at a fixed angle, (ii) first, a rotation of $\mathbf{M}_R$ with constant magnitude of $\mathbf{M}_R$, then decay of $\mathbf{M}_R$, and (iii) rotation and decay of $\mathbf{M}_R$ combined. Over which decay channel the relaxation of $\mathbf{M}_R$ occurs depends on the relative height of the pinning barriers. The present data suggest that the relaxation behavior of $M_{R,ab}$ and $M_{R,c}$ are strongly correlated. The rotation of $\mathbf{M}_R$ is a manifestation of a microscopic rotation of individual flux lines or bundles of flux lines toward the c direction ($T<40$ K) or ab plane ($T>50$ K), respectively. This interpretation is supported by the fact that for $T<40$ K and increasing orientation angle θ, the effective activation energy in the c direction, $U_{0,c}$ increases, whereas in the ab plane a decrease of the activation energy $U_{0,ab}$ is observed (Table II).

The most striking result of this investigation is the unexpected temperature and time behavior of the angle Ψ. It is evident from Figs. 4 and 5 that there are two distinct temperature regions, where the behavior of Ψ is quite different. Below 40 K, Ψ decreased with increasing temperature and time (rotation of $\mathbf{M}_R$ toward the c direction). Above 40 K, on the other hand, Ψ increased with increasing temperature and time (rotation of $\mathbf{M}_R$ toward the ab plane). Similar relaxation experiments were previously performed in single-crystal $Bi_2Sr_2CaCu_2O_8$ by Tuominen *et al.*[13] In contrast to our results, they found that over the entire temperature range, M_R always aligns with the c direction, even for large $\theta \simeq 90°$, which leads us to conclude that there is a significant difference in the vortex structure and dynamics of $YBa_2Cu_4O_8$ and

$Bi_2Sr_2CaCu_2O_7$.

A common feature of all cuprate superconductors is their short coherence length ξ_c, which, at low temperatures may even become smaller than the spacing d between the superconducting CuO_2 layers. When ξ_c is sufficiently smaller than d the system has essentially quasi-2D character. With rising temperature ξ_c increases, and for $\xi_c(T_{co}) \simeq d/\sqrt{2}$ a crossover from 2D to 3D behavior should occur at the crossover temperature T_{co}, which is given by the relation,[9,8]

$$\frac{T_{co}}{T_c} \simeq 1 - \frac{2}{\gamma^2}[\xi_{ab}(0)/d]^2 , \quad (8)$$

where γ denotes the anisotropy parameter, and $\xi_{ab}(0)$ is the in-plane coherence length. For $YBa_2Cu_4O_8$ [$\xi_{ab} \simeq 4$ nm, $d = 1.06$ nm (Ref. 14), $\gamma \simeq 10$ (Refs. 14,15)], Eq. (8) predicts a crossover for $T_{co} \simeq 45-55$ K. To our knowledge no evidence for such a crossover from relaxation experiments has been given so far. It is suggested that the unusual temperature and time behavior of Ψ (Figs. 4 and 5) is associated with a dimensional crossover from $2D$ to $3D$. In the low-temperature region $\mathbf{M}_R$ relaxes toward the c direction for all orientation angles. This behavior was previously observed in single-crystal $Bi_2Sr_2CaCu_2O_3$ (Ref. 13) and may be interpreted in the framework of a simplified pancake model, as suggested in Ref. 13. For arbitrary angles, the pancake vortices in adjacent layers form flux lines parallel to the external field, which align parallel to the c axis when the field is turned off through a thermally activated process indicated in the present experiments. Above 40 K the system behaves more like a 3D anisotropic superconductor, and $\mathbf{M}_R$ turns toward the ab plane (Fig. 5). This is most pronounced for high orientation angles. As mentioned in Sec. III, the relaxation rate S_c for $\theta = 88°$ exhibits an unusual temperature behavior (Fig. 3), which may be associated with two different effective pinning barriers (Table II). In the context of the proposed 2D to 3D transition, we note that above 40 K, where the system has 3D character, $S_c(T)$ increases very fast and almost in a linear way, while $S_{ab}(T)$ is decreasing. This clearly reflects the observed rotation of $\mathbf{M}_R$ away from the c direction. We therefore conclude, that, in contrast to the quasi-2D case for large orientation angles the flux lines tend to line up parallel to the ab plane after the external magnetic field has been removed. In summary, the experimental results and the simple arguments given above are consistent with a possible crossover from 2D to 3D behavior in $YBa_2Cu_4O_8$.

ACKNOWLEDGMENTS

We would like to thank F. Waldner, P. Erhart, and V. B. Geshkenbein for many helpful and stimulating discussions. Furthermore we are grateful to M. Le Blanc for suggestions for future investigations. This work was partly supported by the Swiss National Science Foundation.

[1]V. L. Ginzburg, Zh. Eksp. Teor. Fiz. **23**, 236 (1952).
[2]V. G. Kogan, Phys. Rev. B **24**, 1572 (1981).
[3]L. J. Campbell, M. N. Doria, and V. G. Kogan, Phys. Rev. B **38**, 2439 (1988).
[4]V. G. Kogan, N. Nakagawa, and S. L. Thiemann, Phys. Rev. B **42**, 2631 (1990).
[5]J. R. Clem, Phys. Rev. B **43**, 7837 (1991).
[6]L. N. Bulaevaskii, M. Ledvij, and V. G. Kogan, Phys. Rev. B **46**, 366 (1992).
[7]M. Tachiki, T. Toyama, and S. Takahasi, Physica C **185-189**, 303 (1991).
[8]P. H. Kes, J. Aarts, V. M. Vinocur, and C. J. van der Beek, Phys. Rev. Lett. **64**, 1063 (1990).
[9]W. E. Lawrence and S. Doniach, in *Proceedings of the Twelfth International Conference on Low-Temperature Physics* (Kyoto, Japan, 1970), edited by E. Kanda (Keigaku, Tokyo, 1971), p. 361
[10]D. E. Farrell, J. P. Rice, D. M. Ginsberg, and J. Z. Liu, Phys. Rev. Lett. **64**, 1573 (1990).
[11]T. Schneider and A. Schmidt, Phys. Rev. B **47**, 5915 (1993).
[12]C. S. L. Ghun, G. G. Zheng, J. L. Vicent, and I. K. Schuller, Phys. Rev. B **29**, 4915 (1984).
[13]M. Tuominen and A. M. Goldman, Y. C. Chang, and P. Z. Jiang, Phys. Rev. B **42**, 8740 (1990).
[14]J. C. Martinez, Ph.D. thesis, University of Joseph Fourier Grenoble, 1991.
[15]D. Zech, diploma thesis, University of Zürich, 1991, available on request.
[16]J. Karpinski, E. Kaldis, E. Jilek, S. Rusiecki, and B. Bucher, Nature (London) **336**, 660 (1988).
[17]J. Karpinski, E. Kaldis, S. Rusiecki, E. Jilek, P. Fischer, P. Bordet, C. Chaillont, J. Chenevas, J. L. Hodeau, and M. Marezio, J. Less-Common Met. **150**, 129 (1989).
[18]E. Kaldis, J. Karpinski, S. Rusiecki, B. Bucher, K. Conder, and E. Jilek, Physica C **185-189**, 190 (1991).
[19]P. W. Anderson, Phys. Rev. Lett. **9**, 309 (1962).
[20]C. W. Hagen, R. Griessen, and E. Salomons, Physica C **157**, 199 (1989).
[21]C. W. Hagen and R. Griessen, Phys. Rev. Lett. **62**, 2857 (1989).
[22]K. A. Müller, M. Takashige, and J. G. Bednorz, Phys. Rev. Lett. **58**, 1143 (1987).
[23]P. Erhart, B. Senning, S. Mini, L. Fransioli, F. Waldner, J. E. Drumheller, A. M. Portis, E. Kaldis, and S. Rusiecki, Physica C **185-189**, 2233 (1991).
[24]C. Rossel, E. Sandvold, M. Sergent, R. Chevrel, and M. Potel, Physica C **165**, 233 (1990).
[25]D. Zech *et al.* (unpublished).
[26]V. N. Zavaritskii and N. V. Zavaritskii, Pis'ma Zh. Eksp. Teor. Fiz. **54**, 335 (1991) [Sov. Phys. JEPT Lett. **54**, 330 (1991)].